Elemantal sulfur and acetate can support life of a novel strictly anaerobic haloarchaeon

Sorokin, D.Y.; Kublanov, I.V.; Gavrilov, S.N.; Rojo, D.; Roman, P.; Golyshin, P.N.; Slepak, V.Z.; Smedile, F.; Ferrer, M.

DOI
10.1038/ismej.2015.79

Publication date
2016

Document Version
Accepted author manuscript

Published in
The ISME Journal: multidisciplinary journal of microbial ecology

Citation (APA)
Sorokin, D. Y., Kublanov, I. V., Gavrilov, S. N., Rojo, D., Roman, P., Golyshin, P. N., Slepak, V. Z., Smedile, F., & Ferrer, M. (2016). Elemantal sulfur and acetate can support life of a novel strictly anaerobic haloarchaeon. *The ISME Journal: multidisciplinary journal of microbial ecology*, *10*, 240-252. https://doi.org/10.1038/ismej.2015.79

ORIGINAL ARTICLE

Discovery of the first obligatory anaerobic haloarchaea growing by acetate-dependent elemental sulfur respiration.

Dimitry Y. Sorokin[1,2], Ilya V. Kublanov[1], Sergei N. Gavrilov[1], David Rojo[3], Pawel Roman[4,5], Peter N. Golyshin[6], Vladlen Z. Slepak[7], Francesco Smedile[8], Manuel Ferrer[9], Enzo Messina[8], Violetta La Cono[8] and Michail M. Yakimov[8]

[1]Winogradsky Institute of Microbiology, Russian Academy of Sciences, Moscow, Russia; [2]Department of Biotechnology, Delft University of Technology, Delft, The Netherlands; [3]Center for Metabolomics and Bioanalysis, Faculty of Pharmacy, CEU San Pablo University, Boadilla del Monte, Spain; [4]Sub-department of Environmental Technology, Wageningen University, Wageningen, Netherlands; [5]Wetsus, Centre of Excellence for Sustainable Water Technology, Leeuwarden, Netherlands; [6]School of Biological Sciences, Bangor University, Gwynedd, UK; [7]Department of Molecular and Cellular Pharmacology, University of Miami Miller School of Medicine, Miami, USA; [8]Institute for Coastal Marine Environment, CNR, Messina, Italy; [9]Institute of Catalysis, CSIC, Madrid, Spain.

Correspondence: M Yakimov, Institute for Coastal Marine Environment, IAMC-CNR, Spianata S. Raineri 86, 98122 Messina, Italy.

Email:

Subject Category: Microbial ecology and functional diversity of natural habitats

Topic: Microbial processes and interactions in extreme environments

Keywords: sulfur cycle; hypersaline anoxic habitats; sulfidogenesis; anaerobic acetate oxidation; haloarchaea; metabolome

Running Title: Strict anaerobic acetate-oxidizing S°-reducing haloarchaea

Abstract

Here we report the discovery of strictly anaerobic extremely halophilic euryarchaea that are capable to obtain energy by dissimilatory reduction of elemental sulfur using acetate as the only electron donor and forming sulfide and CO_2 as the only products. This type of respiration has never been observed in hypersaline anoxic habitats. Moreover, this is the first example of such metabolic capability in the entire Archaea domain. We isolated and cultivated these unusual organisms, selecting one representative strain, HSR2, for detailed characterization. Our studies including genome sequencing, transcriptomic, metabolomics and [^{14}C]-bicarbonate assimilation assays revealed that HSR2 oxidized acetate completely via tricarboxylic acid cycle. Anabolic assimilation of acetate occurs via activated glyoxylate bypass and anaplerotic carboxylation. HSR2 possesses sulfurtransferase and an array of membrane-bound polysulfide reductase genes, all of which are expressed during the growth. Our findings call for reevaluation of potential role of haloarchaea in biogeochemistry of hypersaline anoxic habitats.

Introduction

Hypersaline terrestrial and marine brines are often dominated by extremely halophilic euryarchaea, a unique group of Archaea thriving at salt saturation conditions. According to physiological studies of cultivated haloarchaea and genomic information, they are predominantly aerobic heterotrophs (Andrei et al., 2012). There are only a few known examples of facultative anaerobic haloarchaea species capable of growth either by fermentation, or anaerobic respiration using nitrate, fumarate, dimethyl sulfoxide (DMSO) or trimethylamine *N*-oxide (TMAO) as terminal electron acceptors (Oren and Trüper, 1990; Oren, 1991; Antunes *et al*., 2008; Bonete *et al*., 2008; Werner *et al*., 2014). Since these electron acceptors are present at very low concentrations in hypersaline anoxic habitats (Oren, 2011), it might appear that these facultative anaerobes cannot play a significant role in anaerobic environments. Nonetheless, molecular ecology studies demonstrated that highly reduced sulfur-rich hypersaline sediments and salt deposits are inhabited by haloarchaea with no representatives in culture (Walsh *et al*., 2005; Youssef *et al*., 2011). Can these organisms use elemental sulfur, which can be very abundant, as the alternative terminal electron acceptor? This question was addressed several times in the past 30 years (Grant and Ross, 1986; Tindall and Trüper, 1986; Elshahed *et al*., 2004a, 2004b), but no conclusive answer has been found. Acetate is an abundant electron donor and carbon source in anoxic habitats, which accumulates in the absence of high-potential electron acceptors, such as nitrate or Fe(III) (Afshar *et al*., 1998; Kashevi *et al*., 2002; Slobodkina *et al*., 2009). Therefore, anaerobic oxidation of acetate with low potential electron acceptors, such as partially oxidized sulfur compounds, can be an important cross-point of microbiologically

mediated carbon and sulfur cycles. Until now practically nothing is known about these processes in hypersaline habitats.

Here we describe novel strictly anaerobic haloarchaea that grow at 3-5 M NaCl and reduce sulfur using acetate or pyruvate as the only electron donors and forming sulfide (HS^-) and CO_2 as the only products. Our genomic and functional studies reveal unique mechanisms that support this type of anaerobic respiration. Evidence provided by this study allows us to reconsider the biogeochemical role of haloarchaea in carbon and sulfur cycling. Since we were able to isolate these organisms from different hypersaline ecosystems around the world they certainly have ecological significance, indicating that anaerobic archaeal oxidation of acetate is not an exception, occurring in hypersaline lakes of Kulunda Steppe, but rather a common trait of anoxic salt-saturated habitats.

Materials and methods

Origin of samples, enrichments and cultivation conditions

Top 10 cm sediment cores and brine samples were collected from several hypersaline chloride-sulfate lakes located in the Kulunda Steppe (south-western Siberia, Altai region, Russia) (Sorokin *et al*., 2012). Additionally, superficial anoxic sediments were also collected from sulfidic hypersaline lake Lagoona Fuente de Piedra (coordinates: 37°05.717N; 04°47.483E, Malaga, Spain) and from the deep-sea hypersaline lake Medee (coordinates: 34°26.250N; 22°19.783E, Ionian Sea, Eastern Mediterranean, 3105m water depth) (Yakimov *et al*., 2013). The mineral medium used for enrichment and further cultivation of extremely halophilic sulfur reducers contained the following (g l^{-1}): 240 NaCl; 3 K_2HPO_4; 0.5 NH_4Cl; 10 HEPES.

The pH was adjusted to 7.0 by 1 M KOH. After sterilization the medium was supplemented with 5 mmol l^{-1} $MgCl_2 \times 6H_2O$, 1 ml l^{-1} of trace metal solution (Pfennig and Lippert, 1966) and 10 mg l^{-1} of yeast extract. Elemental sulfur flour was sterilized at 110 °C for 30 min as a wet paste and added to approximately 2 g l^{-1}. Cultivation was performed in serum bottles with butyl rubber stoppers. The medium was made anoxic first by "cold boiling" upon evacuation followed by 3 cycles of flushing with argon-evacuation. Anaerobic conditions were achieved by final addition of 0.2 mmol l^{-1} HS^-. Upon 5 cycles of evacuation-flushing with argon, the residual HS^- concentration in the medium was less than 5 µmol l^{-1}. The cultures were incubated at 30-37 °C with periodic shaking of the flasks. The ability for aerobic growth was examined in the same setup, but in the absence of sulfur and sulfide with magnesium supplied in the form of sulfate salt. Air was added by syringe to anoxic medium to the final concentration of 1%. Growth in enrichments was monitored by measuring of HS^- formation using standard methylene blue method (Trüper and Schlegel, 1964). When sulfide reached the concentration of several mmol l^{-1}, the enrichments were sub-cultured 4-6 times after 1:100 dilution. Pure cultures were obtained by serial dilutions and the final isolates were checked microscopically and by 16S rRNA sequencing.

Chemical analyses

After cell removal and acidification of the supernatant to pH 4.0, acetate concentrations were measured by gas chromatography (Chromoteq-Crystall 5000.2 [Russia]; column Sovpol-5, 1 m, detector PID in the range of temperatures between 180 °C and 230 °C). The cells from 1-4 ml culture samples were separated from the brines by centrifugation in 2 ml Eppendorf tubes at 13,000 rpm for 20 min and the

cell pellets were washed with 4 M NaCl solution with pH 5 to remove the cell-bound FeS. After final centrifugation the pellets were stored frozen until further analysis. Cell protein was measured using the Lowry method after removal of soluble sulfides from the solution by centrifugation and FeS from the pellet (by acidic NaCl washing). Polysulfides were analyzed after methylation, in the form of dimethyl polysulfides as described elsewhere (Roman *et al*., 2014). Dimethyl disulfide (DMDS), dimethyl trisulfide (DMTS) and higher dimethyl polysulfanes (Me_2S_4 to Me_2S_8) were subjected to HPLC equipped with a UV detector (Dionex UltiMate 3000RS, USA). Separation was performed with an Agilent column (Zorbax Extend-C18 1.8 µm, 2.1 x 50 mm) at 20 °C; the UV detector was set to 210 nm. The mobile phase initially was 15 vol.% of methanol in water, which at 0.72 min, was switched to a gradient of the methanol concentration reaching 85% at 10 min. During the next 10 min, the conditions were isocratic; in the following 5 min, the methanol concentration decreased to 15%, remaining isocratic for the final 5 min. The flow rate was maintained at 0.371 ml min^{-1} and the injection volume was 1.25 µl. The method for analysis of polysulfide anions requires derivatization of S_x^{2-} using methyl triflate (≥98%, Sigma-Aldrich, Netherlands) to form the more stable dimethyl polysulfanes. After filtration, samples were mixed with 60 µl methyl triflate in methanol-water medium. After the derivatisation step, the internal standard (dibenzo-a,h-anthracene, Supelco Analytical, USA) in benzene (Sigma-Aldrich, Netherlands) was added to a final concentration of 8 mg l^{-1}. The salt precipitates were removed by centrifugation under anaerobic conditions in glass vials at 3,273 x g for 10 min, and the supernatant was analyzed immediately after centrifugation. Determination of the dimethyl polysulfane concentration in each fraction was carried out after oxidation with nitric acid in a high-pressure vessel for 3 hours at 180ºC. The samples were analyzed for their total

sulfur content with an inductively coupled plasma optical emission spectrometer (ICP-OES) (Perkin Elmer, Optima 5300 DV, USA). Commercially available DMTS (Sigma-Aldrich, Netherlands) was used to validate the method for determination of dimethyl polysulfane concentration. The difference between the DMTS concentration of prepared solutions and the results obtained from ICP-OES analysis was below 1.5% in each of the five replicates. Knowing the concentration of dimethyl polysulfanes, a 3-points calibration was performed every time with each new sample series.

RNA isolation and quantitative reverse transcription PCR analysis (Q-RT-PCR)

Q-RT-PCR was used to estimate the abundance of polysulfide reductases, pyruvate:ferredoxin oxidoreductase, isocitrate lyase and malate synthase transcripts. HSR2 cultures were obtained with acetate or pyruvate. Each, 15 - 25 ml sample was filtered (0.22 µm, Millipore) and total RNA was immediately purified using miRVANA kit (Ambion). RNA samples were treated with Turbo DNA-free kit (Ambion Austin, TX, USA) and cDNA synthesis was performed with SuperScript II Reverse Transcriptase (Invitrogen, Carlsbad, CA, USA) according to the manufacture's instruction. The RT reaction was carried out with 100 ng of total RNA in a MasterCycler 5331 Gradient (Eppendorf, Hamburg, Germany). All Q-RT-PCR experiments were performed using an ABI 7500 Fast Real-Time PCR System thermocycler. Specific primers and TaqMan probes were designed using Primer Express® software v.2.0 (Applied Biosystems, USA). TaqMan probes were created only for *psrA* genes. The sequences of primers and TaqMan probes are reported in Supplementary Tables S7A and S7B. 5'-6-FAM and 3'-BHQ1 labeled TaqMan

probes were obtained from Biomers. Samples were tested in triplicates along with "No Template Control" (NTC). The reaction mixtures for Taqman Q-RT-PCR were as follows: 0.8 µM final concentration of each primer, 0.2 µM TaqMan probe, 20 ng of template, 12.5 µl of 2X TaqMan 5 Universal PCR Master Mix (PE Applied Biosystems) and ultrapure water added to a final 25 µl volume. The reactions were performed under the following conditions: 2 min at 50°C followed by 10 min at 95°C, followed by 40 cycles of 15 s at 95°C and 1 min at 60°C. For SYBR® Green Q-RT-PCR approach, initial denaturation was for 5 min at 95°C, followed by 40 cycles of 95°C for 15 s and 60°C for 1 min. Each 25 µl reaction contained 20 ng of template, 12.5 ml of 2X SYBR® Green PCR Master Mix (Applied Biosystems) and 100 nM of each primer. A dissociation protocol was run at the end of each SYBR® Green real-time PCR reaction to verify that only the expected amplification product was generated. Q-RT-PCR amplification was analyzed under automatic setting of the baseline and threshold values and using the relative standard curve method. Standards for all amplifications were prepared using known amounts of cloned target templates. Amplicons were generated by PCR amplification of the target genes from genomic DNA. The resulting amplicons were then purified using the Wizard SV Gel and PCR Clean–up System kit (Promega, Madison, WI, USA), and cloned in pGEM®-T Easy Vector System I (Promega). After cloning, plasmids were extracted using the QIAprep Spin Miniprep kit (Qiagen) and DNA concentrations were measured using a Nanodrop® ND-1000 spectrophotometer. Standard curves were based on serial dilution ranging between 10^7 and 10^1 copies.

[^{14}C]-bicarbonate assimilation

Two replicate gas-tight 100-ml serum vials were filled with 10 ml of acetate- or pyruvate-grown HSR2 cultures (1.1 - 1.5 x 10^7 cells ml^{-1}) and 10 ml of fresh medium. 30 μCi of [^{14}C]-bicarbonate (56.0 mCi mmol l^{-1}, Amersham Italia, Milan, Italy) were then added. Anaerobic conditions were achieved by final addition of 0.2 mmol l^{-1} HS^-. The cultures, correspondingly supplemented with acetate or pyruvate, were incubated for 10 days at 37°C and fixed by formaldehyde added to the final concentration of 2%. Samples were filtered through 0.1 μm polycarbonate filters (Millipore). Filters were washed three times with 10 ml of prefiltered seawater, acidified in an HCl fume hood for 12 h to remove inorganic carbon and air dried before addition of scintillation cocktail for [^{14}C]-counting in a Wallac 1414 analyzer (PerkinElmer, Monza, Italy). The disintegrations per minute (dpm) values were calculated by subtracting the values detected in the [^{14}C]-bicarbonate control with no biomass from the absolute dpm obtained in the culture samples (Yakimov *et al*., 2014).

Genome sequencing and assembly

Sequencing was performed with a Roche 454 GS FLX Ti sequencer (454 Life Sciences, Branford, CT, USA) at Lifesequencing S.L. (Valencia, Spain). In parallel, sequencing was carried out on Illumina HiSeq 2000 platform at BGI (Hong Kong), yielding 5,736,282 paired-reads with an average read length of 101 bp, totalling 579.36 Mbp. Assemblies were performed with Roche Newbler assembler v. 2.5.3 using the default parameters and Velvet v. 1.1. The number of reads accounted to 527,470 sequences with a mean read length of 463.97 bp that provided a total of 244.72 Mbp. The assembly provided a total of 23,721 contigs, where 837 were longer than 500 bp and the N_50 10,833 with the largest contig of 32,349. These

reads were further assembled using both Velvet 1.2.10 (Zebrino, Birney, 2008) and Geneious 7.1 software (http://www.geneious.com/). Gaps between contigs were closed in a conventional PCR-based approach and supported by manual refining with Geneious 7.1 embedded tools, resulting in a fully closed circular chromosome of 2,085,482 bp, and one circular plasmid of 124,256 bp. Together, all sequences provided 151× coverage for HSR2 chromosome and 62× for the plasmid.

Genome annotation

Potential protein-coding genes were analysed by Glimmer 3.02 (Delcher *et al*., 2007), Geneious 7.1 software, NCBI online tool for rRNA and by tRNAScan-SE online tool for tRNA. Operon predictions were performed by the FgenesB online tools (Tyson *et al*., 2004). For each predicted gene, similarity searches were performed by BLAST in Geneious 7.1 against public sequence databases (nr, SwissProt) protein family databases (Pfam) and clusters of orthologous groups (COGs) and then annotated. Finally, annotations were manually curated using the Artemis 15.0 program (Rutherford et al., 2000) and refined for each gene with NCBI blastx against nr database (Altschul et al., 1997). Secreted proteins were predicted with SignalP 4.1 server (http://www.cbs.dtu.dk/services/SignalP/index.php [Petersen *et al*., 2011]). Transmembrane helices were predicted using TMHMM Server v. 2.0 (http://www.cbs.dtu.dk/services/TMHMM/).

Phylogenetic analysis and general predictions

16S rRNA gene phylogeny of the HSR strains was inferred from a 16S rRNA gene sequence alignment with PAUP*4.b10 using a LogDet/ paralinear distance method. Support for nodes in the tree corresponds to bootstrap values for 1000

pseudoreplicates. The tree has been arbitrarily rooted on the closest haloarchaea Salt Deposit Clade II (Walsh *et al*., 2005). The complete genomes of 29 haloarchaeal isolates were obtained from NCBI genome database (http://www.ncbi.nlm.nih.gov/sites/genome, see Supplementary Table S1). We selected six single copy genes identified in most archaea genomes (Lloyd *et al*., 2013) to form a group of orthologous proteins, with the following order: COG0052, Ribosomal protein S2; COG0092, Ribosomal protein S3; COG0081, Ribosomal protein L1; COG0090, Ribosomal protein L2; COG0087, Ribosomal protein L3; COG0088, Ribosomal protein L4. We concatenated them maintaining the same order for each haloarchaeal to form sequences ready to be aligned with the Clustal W (Larkin *et al*., 2007) plugin inside Geneious 7.1 software using the IUB DNA weight matrix. The resulted alignment was used for construction of the maximum likelihood (ML) phylogenetic tree using PhyML program version 3.0 (Guindon and Gascuel, 2003) and the Tamura-Nei substitution model. All positions containing gaps and missing data were eliminated. Bootstrap values over 60% were retained and showed in the tree.

The dataset of molybdopterin reductases was chosen as follows: 4 HSR2 molybdopterin oxidoreductases subunits A (HLASFs); 10 best BLAST hits of all four HLASFs were obtained via Uniprot BLAST utility (http://www.uniprot.org/blast/) and 2 databases for each: UniProtKB & UniProtKB-SwissProt. The results were filtered by "complete proteomes only" option. All best hits than were filtered through 0.99 filter using CD-hit utility (http://weizhong-lab.ucsd.edu/cdhit_suite/cgi-bin/index.cgi?cmd=h-cd-hit) (Huang *et al*., 2010) to eliminate duplicates and reduce redundancy. Biochemically characterized sulfur reductase SreA from *Acidianus* ambivalens (Laska *et al*., 2003) was not detected among these best hits as it was

still found in UniProt (not SwissProt) database and more distant than the first 10 HLASFs UniProtKB best hits. Thus, we have added it manually along with its own 10 UniProtKB best hits. The homologous sequences were included to the previous dataset (Duval *et al*., 2008) after removal of partial sequences (ArrA_DesDC; ArrA_DesY5; ArrA_SulBa; ArrA_BacSe; Psr/PhsA_DesDe; AroA_AlcFa). Upon manual removal of duplicates the final dataset consisted of 147 sequences. The dataset was aligned in MEGA6 (Tamura *et al*., 2013) using Muscle. The evolutionary history was inferred by using the Maximum Likelihood method based on the Whelan And Goldman + Freq. model (Whelan and Goldman, 2001). All positions containing gaps and missing data were eliminated. There were a total of 361 positions in the final dataset. The tree with the highest log likelihood (-77939.2454) is shown. The percentages of trees in which the associated taxa clustered together (bootstrap values, 1000 replicates) are shown next to the branches. Evolutionary analyses were conducted in MEGA6. Final processing was done in MacVector (v. 11.1.2).

Analysis of clustered regularly interspaced short palindromic repeats (CRISPR)

Pilercr v1.02 (Edgar, 2007) was used to identify short palindromic repeats and spacers in the genome of strain HSR2, using default parameters. Also, the CRISPRfinder online tool was used for control (Grissa et al., 2007). CRISPR and close relatives Cas protein were identified with BLAST (Altschul *et al*., 1997). Spacer sequences detected in CRISPR system were analyzed in order to find similarity against plasmid, virus and prophage. Using the ACLAME database (Leplae *et al*., 2010), nucleotide sequences were blasted against Plasmid, Virus and Prophages databases separately inside the ALCAME web site (http://aclame.ulb.ac.be/) by default parameter. Moreover, spacer sequences detected by Pilercr v1.02 were

blasted against env_nt blast using Geneious 7.1 software. A portion of the best hit sequences (max bit score) containing the spacers of at least 100 bp was manually compared against nr and nt NCBI databases using blastx and blastn respectively. Only hits with bit score higher than 30 were considered for analysis.

Targeted metabolomic analysis

The presence of 31 chemical species, known to participate in central metabolism of HSR2 including the pyruvate metabolism and the TCA cycle, was quantified in cell extracts obtained from 10 ml cultures, respectively grown on acetate or pyruvate, after independent metabolite extraction as previously described (Kubacka *et al*., 2014). Metabolomic analysis was performed across three complementary platforms including mass spectrometry (MS) with gas (GC) and liquid chromatography (LC) and capillary electrophoresis (CE) separations (GC-QTOF-MS, LC-QTOF-MS and CE-TOF-MS), which were needed to quantify the each of the different chemical species herein analyzed. Table S8 lists the chemical species identified and quantified per technique. Complete descriptions of the sample preparation protocols prior to analysis and analytical methods are extensively described in Supplementary Methods. To ensure the analytical reproducibility in LC-MS and CE-MS, quality controls (QCs) samples were required to analyze throughout the analytical runs in periodic intervals of time in order to monitor the variation of the signal across time and at the beginning of the sequence to stabilize the system (Dunn *et al*., 2011). QCs samples were independently prepared for LC-MS and CE-MS by pooling and mixing equal volume of each sample (see Supplementary Methods for full details). The resulting data files (GC-QTOF-MS, LC-ESI-QTOF-MS, CE-TOF-MS) files were cleaned of background noise and unrelated ions by Mass Hunter Qualitative Analysis

software (B.05.00, Agilent). This tool was used to look for the target list of the compounds to be identified and quantified. The corresponding peak area of each target compound (using the most appropriate technique and monoisotopic masses) was used to calculate the average and the coefficient of variation between the two technical replicates.

Data deposition

16S rRNA gene sequences reported in this paper have been deposited in the GenBank database (accession no. from KM875607 to KM875612). The genome sequence of strain HSR2 has been submitted to GenBank (accession numbers CP008874 [circular chromosome] and CP008875 [circular plasmid]).

Results

Isolation of haloarchaeal strains HSR2, HSR3, HSR4, HSR5, HSR7 and M27-SA2 and global distribution of related organisms

Active sulfur reduction was repeatedly observed in mixed anaerobic sulfur-rich sediment samples from the Kulunda Steppe hypersaline lakes (Altai, Russia) (Sorokin et al., 2012). To explore the microbiology of this process in details, we isolated four axenic sulfidogenic acetate-oxidizing haloarchaeal cultures designated HSR2, HSR3, HSR4 and HSR5. The nearly identical 16S rRNA gene sequences of these strains demonstrated that they belong to a single genetic species. Comparative phylogenetic analysis placed them within the family *Halobacteriaceae* as a novel lineage with 92-93% sequence homology to the genera *Halarchaeum* and *Halobacterium* (Fig. 1 and Supplementary Fig. S1). Together with uncultivated

members of the ancient salt deposit cluster SD-II (Walsh *et al*., 2005), these isolates form a new monophyletic group. In phylogenetic tree, constructed on the basis of 6 conserved proteins from 29 available haloarchaeal genomes, the positioning of HSR2 in the Clade III of the Class *Halobacteria* was strongly supported (Supplementary Fig. S2). This clade previously consisted of only two members, *Halobacterium* sp. NRC-1 and *Halobacterium* sp. DL1. Our HSR isolates are 97-98% similar to the available cloned 16S rRNA gene sequences of uncultured haloarchaea obtained from hypersaline anoxic soils, brines and sediments around the world (Supplementary Fig. S3). To confirm that this unusual type of anaerobic haloarchaea are indeed widely distributed, we isolated similar acetate-oxidizing S^0-reducing haloarchaea from anoxic hypersaline sediments of Lagoona Fuente de Piedra (Malaga, Spain) and of the deep-sea hypersaline lake Medee (Ionian Sea, Eastern Mediterranean, water depth 3105 m) designated HSR7 and M27-SA2, respectively. Along with the Kulunda isolates, all these strains formed a novel genus-level lineage within the family *Halobacteriales*. We propose to name this taxon "*Halanaeroarchaeum sulfurireducens".*

General physiological description of the strain HSR2

We performed further detailed characterization of the HSR2 isolate, which we chose as the type strain of this physiologically novel group of *Halobacteria*. This organism grew between pH 6.7 and 8.0 (with the optimum at pH 7.2 - 7.5), salinity between 3.0 and 5.0 M NaCl and with the optimum temperature at 40°C. The cells have very thin cell walls, a large nucleoid and a typical haloarchaeal morphology mostly in the form of flat irregular cocci and rods (Fig. 2, A and B). The biomass visually lacked any of light-scavenging pigments present in most of the *Halobacteria*. Fermentative growth

on lactate and sugars was not observed. No anaerobic growth was observed on peptone and yeast extract both in absence and in the presence of elemental sulfur. The isolate has a very limited metabolic profile restricted to acetate and pyruvate as the sole source of carbon and energy. Among various electron acceptors tested either with acetate or pyruvate (anthraquinone-2,6-disulfonate, arsenate, arsenite, DMSO, ferrihydrite, fumarate, manganese [IV] oxide, nitrate, nitrite, nitrous oxide, selenate, selenite, sulfate, sulfite, tetrathionate, thiosulfate and TMAO), growth occurred only with elemental sulfur. The overall reaction of S°-dependent acetate oxidation is a low energy-yielding conversion with the following stoichiometry and standard Gibbs energy yield (Thauer, 1988):

$$CH_3COO^- + 4S° + H^+ + 2H_2O \rightarrow 2CO_2(g) + 4H_2S;\ \Delta G°' = -39\ kJ\ mol^{-1}.$$

Growth of HSR2 on acetate and S° resulted in production of approximately 9.10 ± 0.92 mmol l^{-1} HS^- at the expense of 2.50 ± 0.34 mmol l^{-1} consumed acetate (Fig. 2C), which is a near-stoichiometric oxidation. Part of the cell carbon might have also originated from yeast extract present in the medium at low concentration (10 mg l^{-1}). Compared to acetate, growth with pyruvate as the electron donor resulted in lower HS^- formation but higher biomass yield (Fig. 2D).

General features of the HSR2 genome

The whole genome sequence of the HSR2 strain was determined (Supplementary Tables S2-S4 and Supplementary Fig. S4-S8) and its general features are discussed in Supplementary Discussion. The genome is composed of two circular replicons: a chromosome of 2,085,482 base pairs (bp) and a 124,256-bp plasmid correspondingly containing 2,111 and 117 predicted protein-encoding open reading frames. Out of all these coding sequences, 1,336 chromosomal (63.3%) and only 23

plasmid genes (19.7%) were affiliated with known COGs. The genome harbours 47 tRNA genes and one complete rRNA operon. One gene cluster encoding Clustered Regularly Interspaced Short Palindromic Repeats (CRISPRs) and CRISPR-associated proteins was found in the HSR2 genome. This system is known to be responsible for prokaryotic immunity to phage infection (Deveau and Garneau, 2010). Detailed comparisons revealed particularly high similarity between the HSR2 strain and *Halorhabdus utahensis* with regards to the CRISPR-proteins, the number of repeats and their consensus sequence (Supplementary Fig. S7). Remarkably, these clusters showed no homology between the spacer sequences, likely implying a different history of phage interaction for the isolated strains in their respective environments, regardless of the genomic and structural similarity of these two CRISPR systems.

Genetic determinants of acetate oxidation and respiratory chain

Consistent with narrow specialization of HSR2 in metabolising acetate, its genome contains multiple genes for acetate import, activation, oxidation and assimilation. These include a sodium-acetate symporter (HLASF_0396) of the 2.A.21 family (Saier *et al*., 2014), two ADP-forming acetyl-CoA synthases (operon HLASF_0398-0400), one putative succinyl-CoA:acetate CoA-transferase (HLASF_2086), one pyruvate ferredoxin oxidoreductase (PFOR, HLASF_0492-0493), all enzymes of the TCA cycle, and a complete set of glyoxylate bypass enzymes (see Fig. 3 for details).

In addition to the membrane-bound succinate dehydrogenase (Complex II; HLASF_1576-1579) of the TCA cycle, the Complex I oxidoreductase provides another electron entry point in the HSR2 respiratory chain. Complex I genes were found in many genomes of anaerobic Archaea including *Archaeoglobus*,

Thermoproteus and several methanogens. Only 11 of the 14 Complex I subunits are observed in most of these organisms (Siebers *et al*., 2011). Three other subunits, catalyzing NADH binding and oxidation in complex I of aerobes, are replaced by non-homologous ferredoxin- or F_{420}-oxidizing subunits. Similarly, HSR2 has a complete set of "anaerobic" Complex I genes, located at a single site in the genome (HLASF_1225-1235). The F_{420}-oxidizing NuoF subunit is missing indicating that this organism uses ferredoxins, rather than this cofactor, to funnel electrons into the menaquinone pool. The HSR2 strain has only one ATP synthase operon (HLASF_0205-0213) belonging to H^+-translocating V-type ATPases (Mulkidjanian *et al*., 2008), thus resembling all known haloarchaeal homologues.

The HSR2 genome lacks genes encoding cytochrome *c*-oxidases found in aerobic prokaryotes and any atypical variants of cytochromes found in anaerobic bacteria. Furthermore, the genes coding for another crucial complex of aerobic respiratory electron transfer chain – the cytochrome bc_1 complex – are absent, along with homologues of the alternative Complex III (Refojo *et al*., 2010), confirming the inability of this organism for oxygen respiration. Cytochrome *bd* ubiquinol oxidase, present in HSR2 (HLASF_0492-0493), likely serves for oxygen detoxification, similar to oxidases of other strict anaerobes, such as acetogens and sulfate reducers (Jünemann, 1997). Other candidate proteins involved in oxidative stress protection in HSR2 include a protein homologoius to the bifunctional enzyme catalase/peroxidase from *Haloarcula marismortui* (HLASF_0191) and a putative manganese superoxide dismutase (HLASF_1272).

HSR2 genetic determinants and biochemical challenges of anaerobic respiration on elemental sulfur

With regard to electron acceptor utilization, four operons encoding oxidoreductases of the molybdopterin superfamily were identified in the HSR2 genome (Supplementary Fig. S5). According to the entire operon structures, to the phylogeny of catalytic subunits A and the number of transmembrane regions of subunits C, three of these oxidoreductases were annotated as membrane-bound polysulfide reductases PsrABC (HLASF_0052-0054, HLASF_0694-0696 and HLASF_1287-1285). Concatenated sequences of core subunits of these operons have a strong similarity, suggesting recent duplication events that led to their formation. Phylogenetic analysis of catalytic molybdenum subunits placed HSR2 polysulfide reductases in a distinct haloarchaea-specific cluster, adjacent to the Psr/Phs family (Duval *et al*., 2008) (Fig. 4, Supplementary Fig. S6). Catalytic subunit A phylogeny and core genes organization attribute a fourth operon of molybdopterin oxidoreductase to the clade of tetrathionate reductases. However, as we mentioned above, the HSR2 strain did not grow with tetrathionate.

The analysis of supernatant from a stationary phase HSR2 culture grown with acetate demonstrated the presence of inorganic polysulfides at a total sulfur concentration of 1.3 mmol l^{-1} with a domination of S_4^{2-} (i.e. 0.65 mmol l^{-1} mobolized zero-valent sulfur). The formation of these soluble inorganic polysulfides likely occurred due to spontaneous reaction of elemental sulfur with HS^- (Hedderich et al., 1999). While the initial concentration of HS^- measured in the HSR2 growth medium is very low (5 µmol l^{-1}), its amount increased up to 9.0 mmol l^{-1} HS^- in the stationary phase (Fig. 2C). However, the concentration of polysulfides in neutral condition is low due to chemical instability and therefore their utilization as an electron acceptor still poses biochemical challenges to the sulfur-respiring microorganisms. We proposed that this process may rely on the utilization of a specific polysulfide-binding

carrier protein that represents the actual substrate for the catalytic molybdenum (Mo)-containing PsrA subunit of polysulfide reductases. Indeed, one of the three HSR2 PsrABC operons contains a gene encoding a protein (HLASF_0693) belonging to sulfurtransferase family (Supplementary Fig. S5), which likely plays a role in binding, stabilizing and transferring inorganic polysulfide molecules to PsrA subunit (Klimmek *et al*., 1998) (Fig. 5).

Gene expression, metabolism and [^{14}C]-bicarbonate assimilation during growth of the HSR2 cells

Transcription analysis of genes for catalytic subunits of all four oxidoreductases demonstrated that during growth on acetate and elemental sulfur, *psr*A (HLASF_0694) of the sulfurtransferase-containing operon had the highest expression levels (21.05 ± 3.59 copy cell^{-1}, Supplementary Table S5). Synthesis of pyruvate from acetyl-CoA through a carboxylating reaction catalysed by PFOR was confirmed both by transcriptomic analysis of this enzyme (1.58 ± 0.23 copy cell^{-1}), [^{14}C]-bicarbonate assimilation assay (40 ± 10 ag C cell^{-1} day^{-1}) (Fig. 3, Supplementary Tables S5-S7), and by analysis of the pool of intracellular metabolites, participating in the pyruvate metabolism and the TCa cycle (Supplementary Table S8). Using a metabolomics approach, we confirmed that besides pyruvate, the HSR2 cells use oxaloacetate and 2-oxoglutarate as precursors for biosynthesis (Supplementary Table S8). To replenish them and to avoid depletion of metabolites of the TCA cycle, acetyl-CoA and glyoxylate are likely converted into malate via the glyoxylate bypass (Fig. 3). The expression of isocitrate lyase (10.45 ± 2.42 copy cell^{-1}) and malate synthase (4.75 ± 1.65 copy cell^{-1}) genes during growth on acetate confirmed the likelihood of this reaction (Supplementary Table S5). As

shown by [^{14}C]-labelling experiments, during growth on pyruvate the bicarbonate assimilation was also observed in much higher extent (360 ± 10 ag C cell^{-1} day^{-1}, Supplementary Table S6). This function was evidently taken over by NADP-malic enzyme (HLASF_1723), a sole enzyme apart from the PFOR complex (HLASF_0492-0495), whose activity in the carboxylating direction (Hong and Lee, 2001; Zelle *et al*., 2011) might be involved in anaplerotic assimilation of bicarbonate in HSR2.

Discussion

Hypersaline aquatic environments are abundant worldwide and store nearly as much water as freshwater lakes (Vallentyne, 1972; Hammer, 1986). These hydrological formations, including surficial inland salt lakes, marine coastal marshes, solar salterns and deep-sea brine lakes are often dominated by unique group of Archaea. These extremely halophilic euryarchaea (haloarchaea) have developed a low energy-demanding (so called “salt-in”) strategy to thrive at salt saturation conditions. According to physiological studies and genomic information of cultivated haloarchaea, they are predominantly aerobic heterotrophs. The present work has provided new insights into the molecular mechanisms underlying energy generation and metabolism of this group of prokaryotes. By isolation, cultivation and genome analysis of strictly anaerobic sulfur-respiring acetate-oxidizing haloarchaea we demonstrated that these organisms have a much broader functional capability, which allows them to populate also the anoxic habitats.

Phylogenetically, the strains described here had nearly identical 16S rRNA gene sequences and formed a novel genus-level branch within the family *Halobacteriacea*, with a maximum of 93% sequence similarity to the nearest cultured

members. Closely related strains were numerically dominant microbes in various terrestrial and deep-sea hypersaline anoxic sites around the globe. Thus, it would appear that these strains are very relevant to understanding the functional contribution of haloarchaea to anaerobic carbon and sulfur cycling in salt-saturated environments.

Analysis of the HSR2 genome provided remarkable insights into its unique metabolic capabilities and strategies for survival of this strain under such habitat-specific stress factors as extreme salinity and low solubility of electron acceptor. The main factors that determine whether a certain type of microorganism can live at extreme salinity are the amount of energy generated during its dissimilatory metabolism in combination with the mode of maintaining of osmotically balanced and functional cytoplasm (haloadaptation) (Andrei *et al*., 2012; Oren, 2011; 2013). The haloadaptation impose high energetic costs and limits the number of prokaryotes that can thrive in the dark and anoxic salt-saturated (>250 g l^{-1}) environments where highly exergonic processes, such as photosynthesis, aerobic and nitrate respiration, cannot be operative. This is why at hypersaline anoxic conditions final oxidation of acetate to CO_2 by secondary anaerobes with low-potential electron acceptors, such as sulfur or sulfate, is problematic and has not previously been demonstrated in the entire *Archaea* domain. In that respect, haloarchaea have an advantage over other organism, since they employ a "cheap" mode of haloadaptation based on potassium import (Oren, 2011). Central to the HSR2 metabolism is its ability to anaerobically oxidize acetate, which is the main recalcitrant intermediate of anaerobic degradation of organic matter. Using elemental sulfur as terminal electron acceptor, HSR2 oxidizes acetate completely, converting it to CO_2 and H_2O. Hitherto, this type of respiration was described for a very limited number of non-halophilic anaerobic

acetate-oxidizing bacterial species (Rabus *et al*., 2006). In all biochemically and genetically characterized organisms of this functional group, acetate is activated via ATP-dependent acetyl-CoA synthase and oxidized via the tricarboxylic acid (TCA) cycle. HSR2 appears to be no exception, as its genome contains all enzymes of the classical TCA cycle. On the basis of the genomic, transcriptomic, metabolomics and [^{14}C]-bicarbonate assimilation analyses, we demonstrated that HSR2 strain developed multiple anabolic strategies to grow on acetate as the sole electron donor and carbon source. Specifically, acetate assimilation in HSR2 requires the synthesis of acetyl-CoA and the contemporary activity of pyruvate ferredoxin oxidoreductase (PFOR) complex to produce pyruvate and the enzymes of glyoxylate bypass to produce malate. As determined by [^{14}C]-labeling experiments, anaplerotic fixation of CO_2 through a carboxylating reaction, catalyzed by PFOR, occurred at the rates 0.04 ± 0.01 fg C cell^{-1} day^{-1}. During growth on pyruvate the anaplerotic assimilation of bicarbonate in HSR2 is catalyzed by NADP-malic enzyme, working in the carboxylating direction.

Our studies revealed that oxidation of acetate is accomponied by a near stoichiometric production of sulfide. The use of elemental sulfur as the terminal electron acceptor must require a sophisticated suite of energy-conserving enzymes. Indeed, HSR2 genome harbors three operons encoding membrane-bound polysulfide reductases PsrABC and, according to gene transcription studies, all of them are expressed during this type of respiration. Solubility of elemental sulfur in water at neutral pH values is extremely low (less than 160 nmol l^{-1}) and, therefore, S° can hardly be used as the electron acceptor without any adaptive implementations (Klimmek *et al*., 1998). However, in the presence of sulfide a significant amount of S° is transformed into soluble inorganic polysulfide (Hedderich *et al*., 1999). One of the

mechanisms of its utilization as terminal acceptor is described for bacterial sulfur reducers *Wolinella succinogenes* and *Nautilia profundicola* (Klimmek *et al*., 1998; Campbell *et al*., 2009). It relies on activity of a periplasmic sulfurtransferase/ rhodanese-like protein (Sud), which acts as a polysulfide-binding carrier that represents the actual substrate for the catalytic molybdenum (Mo)-containing subunit PsrA. The Sud of *W. succinogenes* binds up to 10 mol of polysulfide sulfur per one mol of enzyme and drastically increases the activity of polysulfide reductase (Klimmek *et al*., 1998; Hedderich *et al*., 1999). Since the supernatant of a stationary phase HSR2 culture contained 1.3 mmol l^{-1} of polysulfide (S_4^{2-}) sulfur, we suggested that HSR2 could employ a similar strategy. As far as half of the sulfur in S_4^{2-} is present in reduced form, the real zero-valent linear sulfur concentration was 0.65 mmol l^{-1}. As we mentioned above, this polysulfide concentration was measured at the final point of growth when 9 mmol l^{-1} sulfur was reduced to HS^-. Polysulfide (S_4^{2-}) is rapidly decomposed back to sulfur and sulfide at low sulfide concentrations and at neutral pH. Thus, only at such high sulfide concentrations it is possible for polysulfide to be present at mM concentrations. On the other hand, accumulation of sulfide at high concentrations inhibits further growth of HSR2. Therefore, the organism must balance between low availability of linear sulfur at low sulfide concentrations (beginning of growth) and better availability of sulfur at toxic concentrations of sulfide.

The analysis of the HSR2 genome revealed the presence of sulfurtransferase, apparently playing a crucial role in the process of insoluble sulfur mobilization at the beginning of growth. Compared to the Sud protein of *W. succinogenes,* which contains only one sulfur-binding domain and needs dimerization to achieve high substrate affinity (Klimmek *et al*., 1998; Rabus *et al*., 2006), the extracellular

HLASF_0693 sulfurtransferase contains 2 homologous domains and may not need dimerization. This might be especially important during the early growth phase of the HSR2 cells when sulfide concentration is at micromolar range. The role of sulfurtransferase may decrease as sulfide/polysulfide concentrations increase during the growth of HSR2.

In summary, our discovery of strictly anaerobic sulfur-respiring haloarchaea calls for reevaluation of *Halobacteria* physiology and their contribution to energy flux and elements cycling in hypersaline anoxic ecosystems. Thermodynamically, anaerobic oxidation of acetate with sulfur as terminal electron acceptor is an exceptionally unfavorable conversion, and for a long time, researchers have been searching for this type of metabolism. Since sulfur-rich anoxic saline habitats were commonplace on early Earth, acetate-dependent anaerobic utilization of elemental sulfur provides new insights into microbial life not only in modern, but possibly in ancient hypersaline anoxic ecosystems.

Conflict of interest

The authors declare no conflict of interest.

Acknowledgements

This work was supported by research fund from European Commission's Program under MicroB3 Project (Contract FP7-OCEAN.2011-2-287589), the Russian Foundation of Basic (13-04-00049, 13-04-40205-N) and the Russian Academy of Science Program "Molecular and Cellular Biology". This work was further funded by grant BIO2011-25012 from the Spanish Ministry of the Economy and Competitiveness." We thank Prof. Coral Barbas (CEU San Pablo University) for her

excellent support in relation to the metabolomics analyses. We sincerely thank Erika Arcadi, Gina LaSpada for technical assistance and Douglas Boettner for his critical reading the manuscript and useful comments.

References

Afshar S, Kim C, Monbouquette HG, Schröder I. (1998). Effect of tungstate on nitrate reduction by the hyperthermophilic archaeon *Pyrobaculum aerophilum*. *Appl Environ Microbiol* **64**: 3004–3008.

Altschul SF, Madden TL, Schäffer AA, Zhang J, Zhang Z, Miller W *et al.* (1997). Gapped BLAST and PSI-BLAST: a new generation of protein database search programs. *Nucleic Acids Res* **25**: 3389–3402.

Andrei AS, Banciu HL, Oren A. (2012). Living with salt: metabolic and phylogenetic diversity of archaea inhabiting saline ecosystems. *FEMS Microbiol Lett* **330:** 1-9.

Antunes A, Taborda M, Huber R, Moissl C, Nobre MF, da Costa MS. (2008). *Halorhabdus tiamatea* sp. nov., a non-pigmented extremely halophilic archaeon from a deep-sea, hypersaline anoxic basin of the Red Sea, and emended description of the genus *Halorhabdus*. *Int J Syst Evol Microbiol* **58**: 215–220.

Bonete MJ, Martínez-Espinosa RM, Pire C, Zafrilla B, Richardson DJ. (2008). Nitrogen metabolism in haloarchaea. *Saline Systems* **4**: 9.

Campbell BJ, Smith JL, Hanson TE, Klotz MG, Stein LY, Lee CK *et al.* (2009). Adaptations to submarine hydrothermal environments exemplified by the genome of *Nautilia profundicola*. *PLoS Genet* **5**: e1000362.

Delcher AL, Bratke KA, Powers EC, Salzberg SL. (2007). Identifying bacterial genes and endosymbiont DNA with Glimmer. *Bioinformatics* **23**: 673–679.

Deveau H, Garneau JE, Moineau S. (2010). CRISPR/Cas system and its role in phage-bacteria interactions. *Annu Rev Microbiol* **64**: 475–493.

Dunn WB, Broadhurst D, Begley P, Zelena E, Francis-McIntyre S, Anderson N *et al.* (2011). Procedures for large-scale metabolic profiling of serum and plasma using gas chromatography and liquid chromatography coupled to mass spectrometry. *Nat Protoc* **6**: 1060–1083.

Duval S, Ducluzeau AL, Nitschke W, Schoepp-Cothenet B. (2008). Enzyme phylogenies as markers for the oxidation state of the environment: the case of respiratory arsenate reductase and related enzymes. *BMC Evol Biol* **8**: 206.

Edgar RC. (2007). PILER-CR: fast and accurate identification of CRISPR repeats. *BMC Bioinformatics* **8**: 18.

Elshahed MS, Najar FZ, Roe BA, Oren A, Dewers TA, Krumholz LR *et al.* (2004a). Survey of archaeal diversity reveals an abundance of halophilic Archaea in a low-salt, sulfide- and sulfur-rich spring. *Appl Environ Microbiol* **70**: 2230–2239.

Elshahed MS, Savage KN, Oren A, Gutierrez MC, Ventosa A, Krumholz LR *et al.* (2004b). *Haloferax sulfurifontis* sp. nov., a halophilic archaeon isolated from a sulfide- and sulfur-rich spring. *Int J Syst Evol Microbiol* **54**: 2275–2279.

Grant WD, Ross HNM. (1986). The ecology and taxonomy of *Halobacteria*. *FEMS Microbiol Rev* **39**: 9–15.

Grissa I, Vergnaud G, Pourcel C. (2007). CRISPRFinder: a web tool to identify clustered regularly interspaced short palindromic repeats. *Nucleic Acids Res* **35**: W52–W57.

Guindon S, Gascuel O. (2003). A simple, fast, and accurate algorithm to estimate large phylogenies by maximum likelihood. *Syst Biol* **52**: 696–704.

Hammer UT. (1986). Saline lake ecosystems of the world. Dr. W. Junk Publishers, P.O. Box 163, 3300 AD Dordrecht, The Netherlands, 616p.

Hedderich R, Klimmek O, Kröger A, Dirmeier R, Keller M, Stetter KO *et al.* (1999). Anaerobic respiration with elemental sulfur and with disulfides. *FEMS Microbiol Rev* **22**: 353–381.

Hong SH, Lee SY. (2001). Metabolic flux analysis for succinic acid production by recombinant *Escherichia coli* with amplified malic enzyme activity. *Biotechnol Bioeng* **74**: 89–95.

Huang Y, Niu B, Gao Y, Fu L, Li W. (2010). CD-HIT Suite: a web server for clustering and comparing biological sequences. *Bioinformatics* **26**: 680–682.

Jünemann S. (1997). Cytochrome bd terminal oxidase. *Biochim Biophys Acta* **1321**: 107–127.

Kashefi K, Tor JM, Holmes DE, Gaw Van Praagh CV, Reysenbach AL, Lovley DR *et al.* (2002). *Geoglobus ahangari* gen. nov., sp. nov., a novel hyperthermophilic archaeon capable of oxidizing organic acids and growing autotrophically on hydrogen with Fe(III) serving as the sole electron acceptor. *Int J Syst Evol Microbiol* **52**: 719–728.

Klimmek O, Kreis V, Klein C, Simon J, Wittershagen A, Kröger A *et al.* (1998). The function of the periplasmic Sud protein in polysulfide respiration of *Wolinella succinogenes*. *Eur J Biochem* **253**: 263–269.

Kubacka A, Diez MS, Rojo D, Bargiela R, Ciordia S, Zapico I *et al.* (2014). Understanding the antimicrobial mechanism of TiO_2-based nanocomposite films in a pathogenic bacterium. *Sci Rep* **4**: 4134.

Larkin MA, Blackshields G, Brown NP, Chenna R, McGettigan PA, McWilliam H *et al.* (2007). Clustal W and Clustal X version 2.0. *Bioinformatics* **23**: 2947–2948.

Laska S, Lottspeich F, Kletzin A. (2003). Membrane-bound hydrogenase and sulfur reductase of the hyperthermophilic and acidophilic archaeon *Acidianus ambivalens*. *Microbiology* **149**: 2357–2371.

Leplae R, Lima-Mendez G, Toussaint A. (2010). ACLAME: a CLAssification of Mobile genetic Elements, update 2010. *Nucleic Acids Res* **38**: D57–D61.

Lloyd KG, Schreiber L, Petersen DG, Kjeldsen KU, Lever MA, Steen AD *et al.* (2013). Predominant archaea in marine sediments degrade detrital proteins. *Nature* **496**: 215–218.

Mulkidjanian AY, Galperin MY, Makarova KS, Wolf YI, Koonin EV. (2008). Evolutionary primacy of sodium bioenergetics. *Biol Direct* **3**: 13.

Oren A, Trüper HG. (1990). Anaerobic growth of halophilic archaeobacteria by reduction of dimethylsulfoxide and trimethylamine N-oxide. *FEMS Microbiol Lett* **70**: 33–36.

Oren A. (1991). Anaerobic growth of archaeobacteria by reduction of fumarate. *J Gen Microbiol* **137**: 1387–1390.

Oren A. (2011). Thermodynamic limits to microbial life at high salt concentrations. *Environ Microbiol* **13**: 1908–1923.

Oren A. (2013). Life at high salt concentration. In: Rosenberg E *et al*. (eds.), *The Prokaryotes – prokaryotic pommunities and ecophysiology,* pp.321-440, Springer-Verlag Berlin Heidelberg.

Petersen TN, Brunak S, von Heijne G, Nielsen H. (2011). SignalP 4.0: discriminating signal peptides from transmembrane regions. *Nature Methods* **8**: 785–786.

Pfennig N, Lippert KD. (1966). Über das Vitamin B12-Bedürfnis phototropher Schwefelbakterien. *Arch Mikrobiol* **55**: 245–256.

Rabus R, Hansen TA, Widdel F. (2006). Dissimilatory sulfate- and sulfur-reducing prokaryotes. In: Dworkin M et al. (eds), *The Prokaryotes – A handbook on the biology of bacteria,* **2**: 659–768, Springer Science+Business Media, Singapore.

Refojo PN, Sousa FL, Teixeira M, Pereira MM. (2010). The alternative complex III: a different architecture using known building modules. *Biochim Biophys Acta* **1797**: 1869–1876.

Roman P, Bijmans MF, Janssen AJ. (2014). Quantification of individual polysulfides in lab-scale and full-scale desulfurisation bioreactors. *Environ Chem* **11**: 702–708.

Rutherford K, Parkhill J, Crook J, Horsnell T, Rice P, Rajandream MA *et al.* (2000). Artemis: sequence visualization and annotation. *Bioinformatics* **16**: 944–945.

Saier MH Jr, Reddy VS, Tamang DG, Västermark A. (2014). The transporter classification database. *Nucleic Acids Res* **42**: D251–D258.

Siebers B, Zaparty M, Raddatz G, Tjaden B, Albers SV, Bell SD *et al.* (2011). The complete genome sequence of *Thermoproteus tenax*: a physiologically versatile member of the *Crenarchaeota*. *PLoS One* **6**: e24222.

Slobodkina GB, Kolganova TV, Querellou J, Bonch-Osmolovskaya EA, Slobodkin AI. (2009). *Geoglous acetivorans* sp. nov., an iron(III)-reducing archaeon from a deep-sea hydrothermal vent. *Int J Syst Bacteriol* **59**: 2880–2883.

Sorokin DY, Zacharova EE, Pimenov NV, Tourova TP, Panteleeva AN, Muyzer G *et al.* (2012). Sulfidogenesis in hypersaline chloride-sulfate lakes of Kulunda Steppe (Altai, Russia). *FEMS Microbiol Ecol* **79**: 445–453.

Tamura K, Stecher G, Peterson D, Filipski A, Kumar S. (2013). MEGA6: Molecular Evolutionary Genetics Analysis version 6.0. *Mol Biol Evol* **30**: 2725–2729.

Thauer RK. (1988). Citric-acid cycle, 50 years on. Modifications and an alternative pathway in anaerobic bacteria. *Eur J Biochem* **176**: 497–508.

Tindall BJ, Trüper HG. (1986). Ecophysiology of the aerobic halophilic archaebacteria. *Syst Appl Microbiol* **7**: 202–212.

Trüper HG, Schlegel HG. (1964). Sulfur metabolism in *Thiorhodaceae*. 1. Quantitative measurements on growing cells of *Chromatium okenii*. *Ant van Leeuwenhoek* **30**: 225–238.

Tyson GW, Chapman J, Hugenholtz P, Allen EE, Ram RJ, Richardson PM *et al.* (2004). Community structure and metabolism through reconstruction of microbial genomes from the environment. *Nature* **428**: 37–43.

Vallentyne JR. (1972). Freshwater supplies and pollution: Effects of the demophoric explosion on water and man. In: Polunin N. (Ed.), *The Environmental Future*, pp. 181-211. Macmillan, London.

Walsh DA, Papke RT, Doolittle WF. (2005). Archaeal diversity along a soil salinity gradient prone to disturbance. *Environ Microbiol* **7**: 1655–1666.

Werner J, Ferrer M, Michel G, Mann AJ, Huang S, Juarez S et al. (2014). *Halorhabdus tiamatea*: proteogenomics and glycosidase activity measurements identify the first cultivated euryarchaeon from a deep-sea anoxic brine lake as potential polysaccharide degrader. *Environ Microbiol* **16**: 2525–2537.

Whelan S, Goldman N. (2001). A general empirical model of protein evolution derived from multiple protein families using a maximum-likelihood approach. *Mol Biol Evol* **18**: 691–699.

Yakimov MM, La Cono V, Slepak VZ, La Spada G, Arcadi E, Messina E *et al*. (2013) Microbial life in the Lake *Medee*, the largest deep-sea salt-saturated formation. *Sci Report* **3:** 3554.

Yakimov MM, La Cono V, Smedile F, Crisafi F, Arcadi E, Leonardi M *et al.* (2014) Heterotrophic bicarbonate assimilation is the main process of de novo organic carbon synthesis in hadal zone of the Hellenic Trench, the deepest part of Mediterranean Sea. *Environm Microb Rep* **6**: 709–722.

Youssef NH, Ashlock-Savage KN, Elshahed MS. (2011). Phylogenetic diversities and community structure of members of the extremely halophilic Archaea (order *Halobacteriales*) in multiple saline sediment habitats. *Appl Environ Microbiol* **78**: 1332–1344.

Zelle RM, Harrison JC, Pronk JT, van Maris AJ. (2011). Anaplerotic role for cytosolic malic enzyme in engineered *Saccharomyces cerevisiae* strains. *Appl Environm Microbiol* **77**: 732–738.

Zerbino DR, Birney E. (2008). Velvet: algorithms for de novo short read assembly using de Bruijn graphs. *Genome Res* **18**: 821–829.

Supplementary Information includes Supplementary Discussion, Supplementary Figures from S1 to S8, Supplementary Tables from S1 to S8, Supplementary Methods and Supplementary References.

Figure Legends

Figure 1 Phylogenetic position of the proposed genus "*Halanaeroarchaeum"* within the family *Halobacteriacea*. Complete haloarchaeal genome sequences available on September 2014 are denoted by red circles, scaffolds - by green squares and contigs – by blue triangles. Haloarchaeal genera known only by 16S rRNA gene sequences are grey. For the genera included in Group I and Group II see table S1. Insert: Detailed phylogenetic tree of *Halanaeroarchaeum*-related sequences produced in this study and available in SILVA database. Similar clones are indicated in parenthesis. Support for nodes in this tree corresponds to bootstrap values for 1000 pseudo-replicates. Only bootstrap values at nodes greater than 75% are displayed as solid circles. The tree has been arbitrarily rooted on the closest haloarchaea Salt Deposit Clade II (SD-II) (*7*). Sequence of *Natronomonas pharaonis* (D87971) was used for outgrouping. Cultivated isolates are denoted in red.

Figure 2 Morphology, cell ultrastructure and growth of strain HSR2. Phase contrast microphotographs show the cells grown on acetate (A), pyruvate (B) and S° and electron micrographs - the cells grown on acetate and S° (C). Growth dynamic in anaerobic cultures with sulfur as electron acceptor either with acetate (D) or pyruvate (E) as energy and carbon source. Standard deviations mean the average data from 3-5 independent cultures.

Figure 3 Pathways of acetate activation and central metabolism in HSR2 as deduced from genome annotation, transcriptomic and metabolimic approaches and [^{14}C]-bicarbonate assimilation assay. Enzymes involved: A. acetyl-CoA synthase (HLASF_0398, HLASF_0400, HLASF_1340); B. putative succinyl-CoA:acetate CoA transferase (HLASF_2086); C. citrate(*si*)-synthase (HLASF_0233, HLASF_1099); D. aconitate hydratase (HLASF_0248); E. NADP-specific isocitrate dehydrogenase (HLASF_1921); F. 2-oxoglutarate:ferredoxin oxidoreductase (HLASF_0747-0748, HLASF_1469-1470); G. succinyl-CoA synthetase (HLASF_1699-1700); H. putative membrane-bound succinate:menaquinone oxidoreductase (HLASF_1576-1579); I. fumarate hydratase (HLASF_1088), J. NAD-dependent malate dehydrogenase (HLASF_0041); K. isocitrate lyase (HLASF_2006); L. malate synthase (HLASF_2007); M. malic enzyme (HLASF_1723); N. pyruvate:ferredoxin

oxidoreductase (HLASF_0492-0495). Pyruvate and metabolites of TCA cycle detected by metabolomics analysis in acetate-grown cells are shown in red. Their relative concentrations, normalized as mV μg^{-1} cell protein, shown in parenthesis. The details on targeted metabolomics analysis are given in the Table S8. Metabolites likely participating in assimilation pathways are underlined. Gene transcripts, detected and quantified by Q-RT-PCR transcriptomic analysis (Supplementary Table S5), are denoted as blue circles.

Figure 4 Phylogenetic tree of molybdopterin oxidoreductase catalytic subunits PsrA. Polysulfide reductase/thiosulfate reductase (Psr/Phs) clade marked in yellow. Other abbreviations used: arsenite oxidases (Aro); arsenate reductases (Arr); dimethylsulfoxide/trimethylamine-N-oxide reductases (DMSO/TMAO); formate dehydrogenases (Fdh); periplasmic nitrate reductases (Nap); membrane-bound nitrate/perchlorate reductases (Nar/Pcr); assimilatory nitrate reductases (Nas); tetrathionate reductases (Ttr); unknown reductases (Unk). *Bacteria* highlighted in black, *Crenarchaeota* in blue, *Euryarchaeota* in green and *Halobacteria* in pink (see Supplementary Figure S6 for full details).

Figure 5 Proposed pathways for sulfur metabolism and energy generation in HSR2, deduced from physiological and genomic data. Enzymes are labeled with numbers of ORFs. The central intermediate in the sulfur pathway is polysulfide, which is predicted to be used as the terminal electron acceptor for energy conservation by a multiple polysulfide reductases under salt saturation conditions at close to neutral pH values. This process likely involves a polysulfide carrier (HLASF_0693) similar to the sulfurtransferase of *Wolinella succinogenes*. Enzymes involved in sulfur metabolism are shown in yellow, Complex I (HLASF_1576-1579) and Complex II (HLASF_1225-1235) are pink.

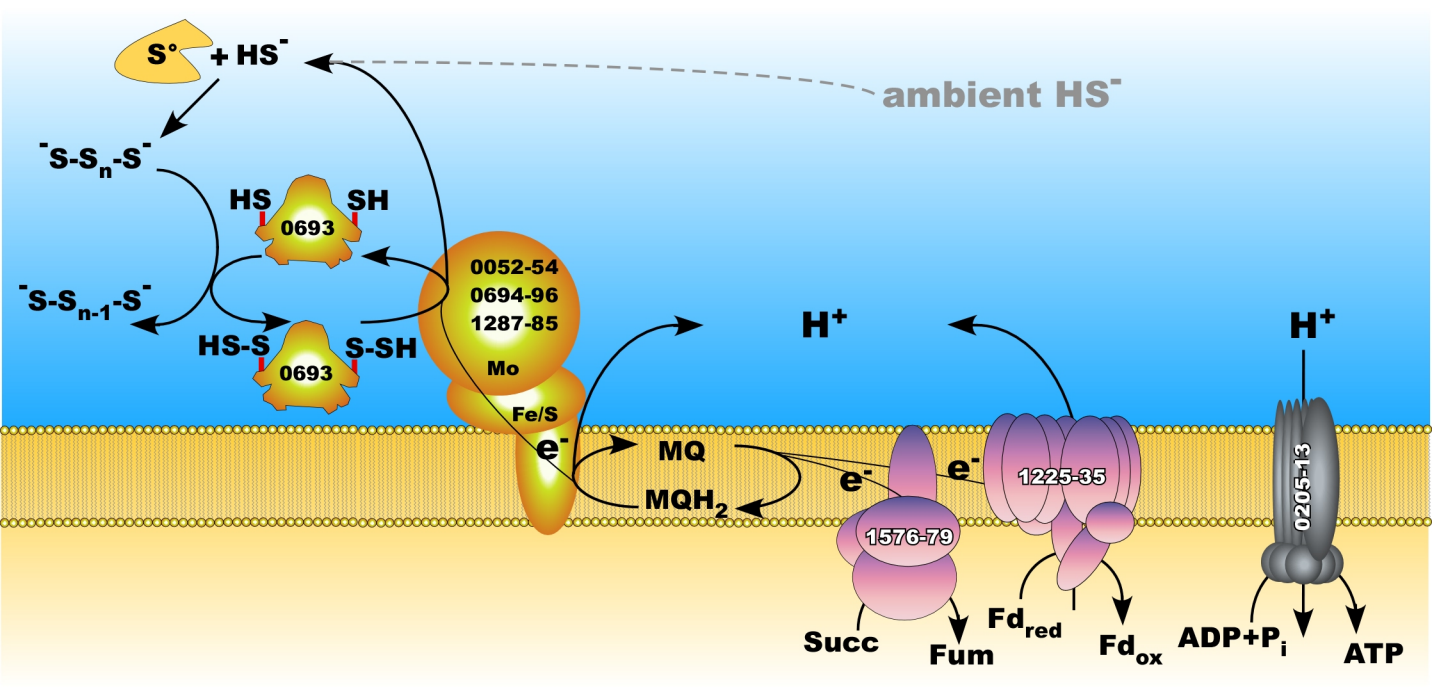
S° + HS⁻
ambient HS⁻
⁻S-Sn-S⁻
HS
SH
0693
⁻S-Sn-1-S⁻
HS-S
S-SH
0693
0052-54
0694-96
1287-85
Mo
Fe/S
e⁻
MQ
MQH2
H+
e⁻
e⁻
1225-35
1576-79
Succ
Fum
Fdred
Fdox
H+
0205-13
ADP+Pi
ATP

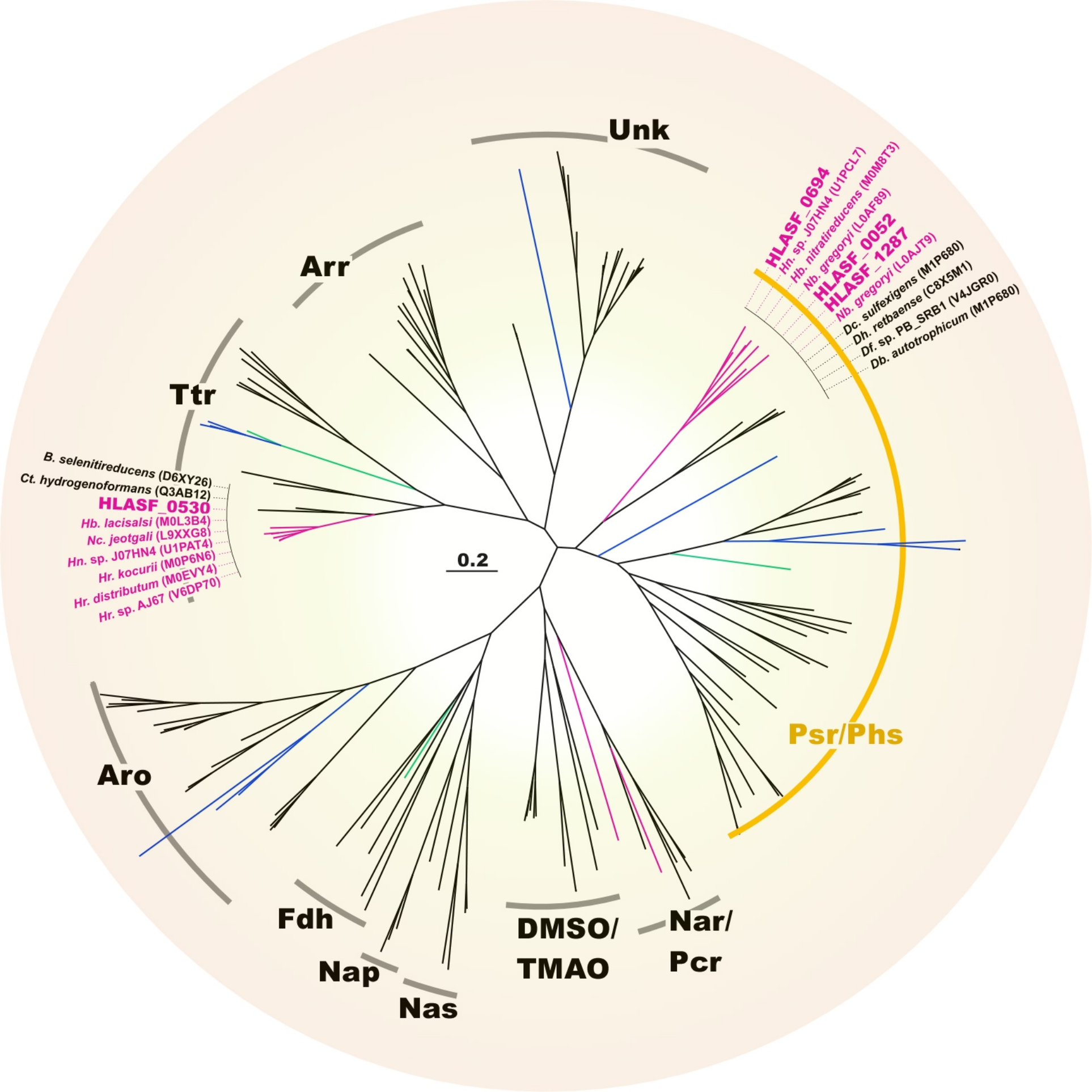
Unk
Arr
Ttr
Aro
Fdh
Nap
Nas
DMSO/
TMAO
Nar/
Pcr
Psr/Phs
0.2
HLASF_0694
Hn. sp. J07HN4 (U1PCL7)
Hb. nitratireducens (M0M8T3)
Nb. gregoryi (L0AF89)
HLASF_0052
HLASF_1287
Nb. gregoryi (L0AJT9)
Dc. sulfexigens (M1P680)
Dh. retbaense (C8X5M1)
Df. sp. PB_SRB1 (V4JGR0)
Db. autotrophicum (M1P680)
B. selenitireducens (D6XY26)
Ct. hydrogenoformans (Q3AB12)
HLASF_0530
Hb. lacisalsi (M0L3B4)
Nc. jeotgali (L9XXG8)
Hn. sp. J07HN4 (U1PAT4)
Hr. kocurii (M0P6N6)
Hr. distributum (M0EVY4)
Hr. sp. AJ67 (V6DP70)

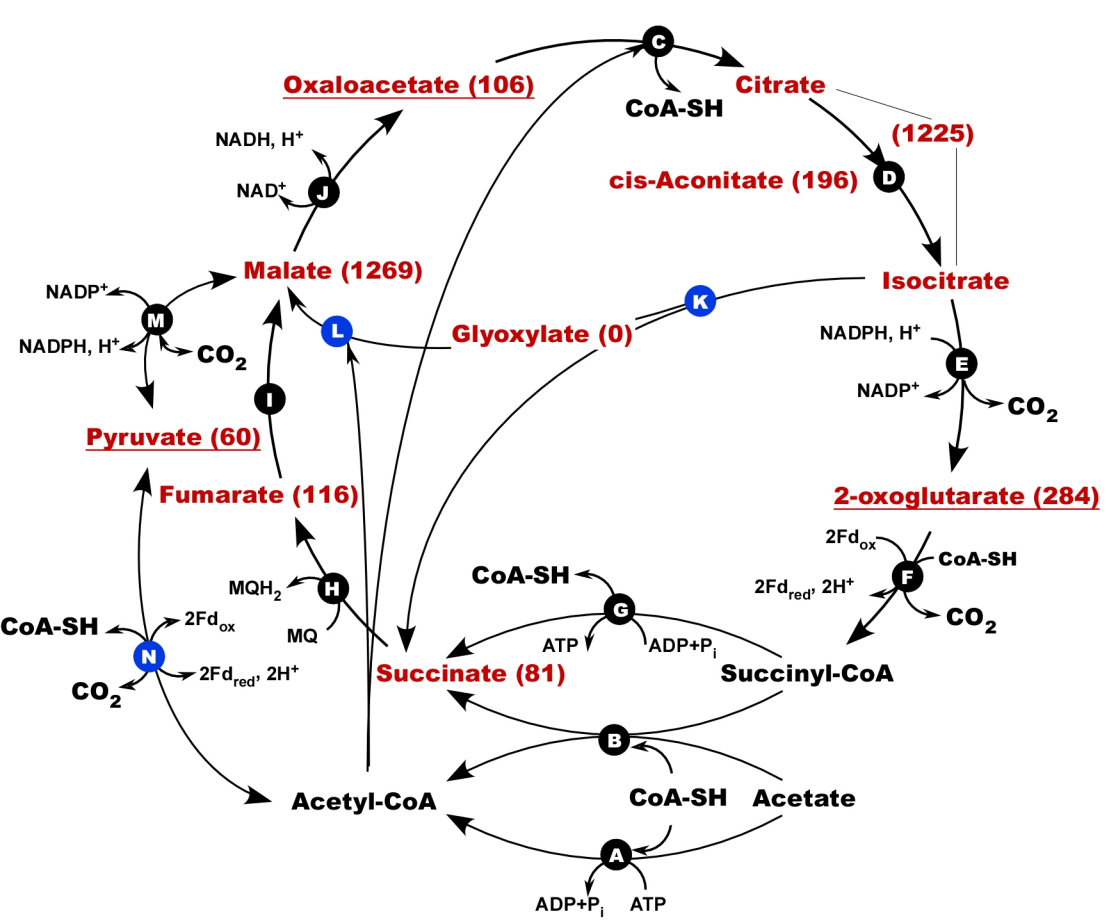
Oxaloacetate (106)
C
CoA-SH
Citrate
(1225)
NADH, H+
NAD+
J
cis-Aconitate (196)
D
Malate (1269)
Isocitrate
NADP+
M
NADPH, H+
CO2
L
Glyoxylate (0)
K
NADPH, H+
E
NADP+
CO2
Pyruvate (60)
I
2-oxoglutarate (284)
Fumarate (116)
2Fdox
CoA-SH
F
2Fdred, 2H+
CO2
MQH2
H
CoA-SH
G
MQ
ATP
ADP+Pi
CoA-SH
2Fdox
N
Succinate (81)
Succinyl-CoA
CO2
2Fdred, 2H+
B
Acetyl-CoA
CoA-SH
Acetate
A
ADP+Pi
ATP

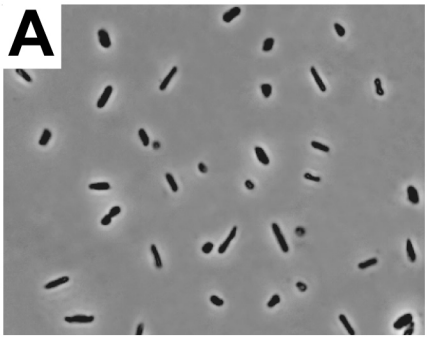
A
10 µm

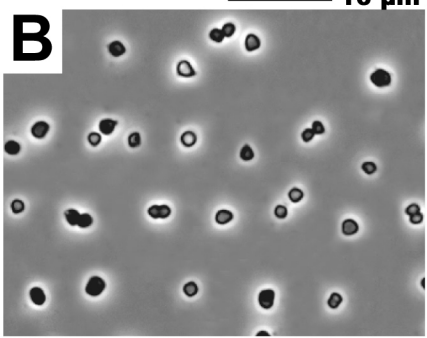
B

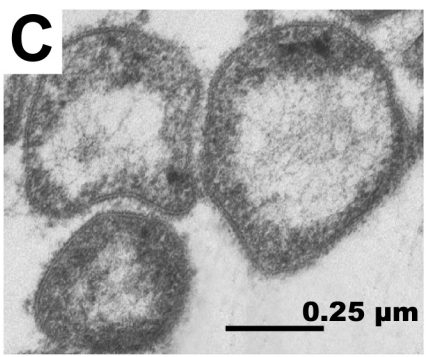
C
0.25 µm

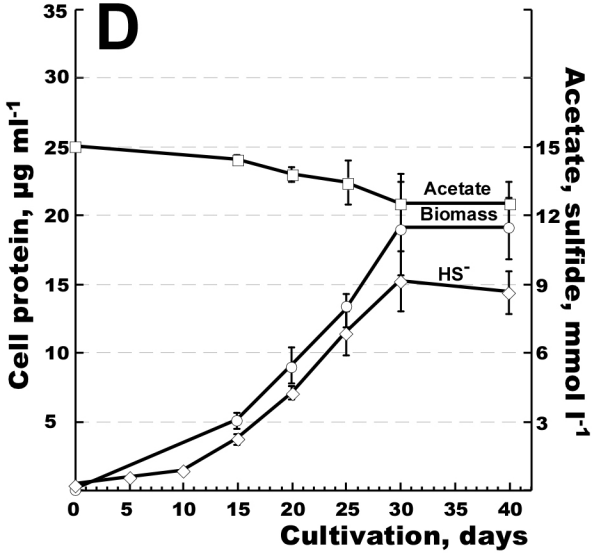
D
Cell protein, µg ml-1
Acetate, sulfide, mmol l-1
Acetate
Biomass
HS-
Cultivation, days

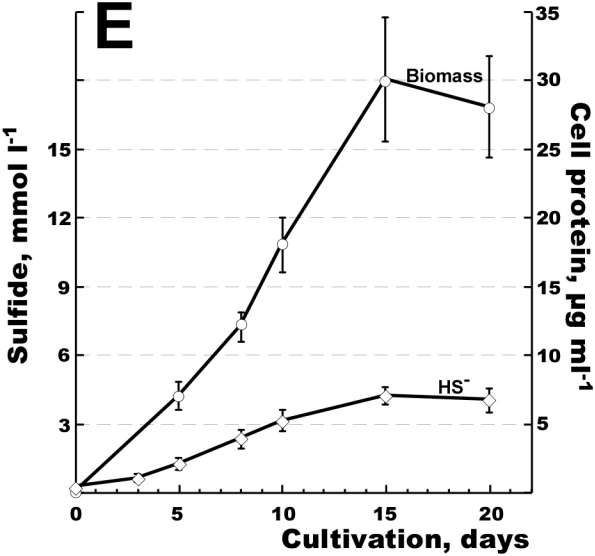
E
Sulfide, mmol l-1
Cell protein, µg ml-1
Biomass
HS-
Cultivation, days

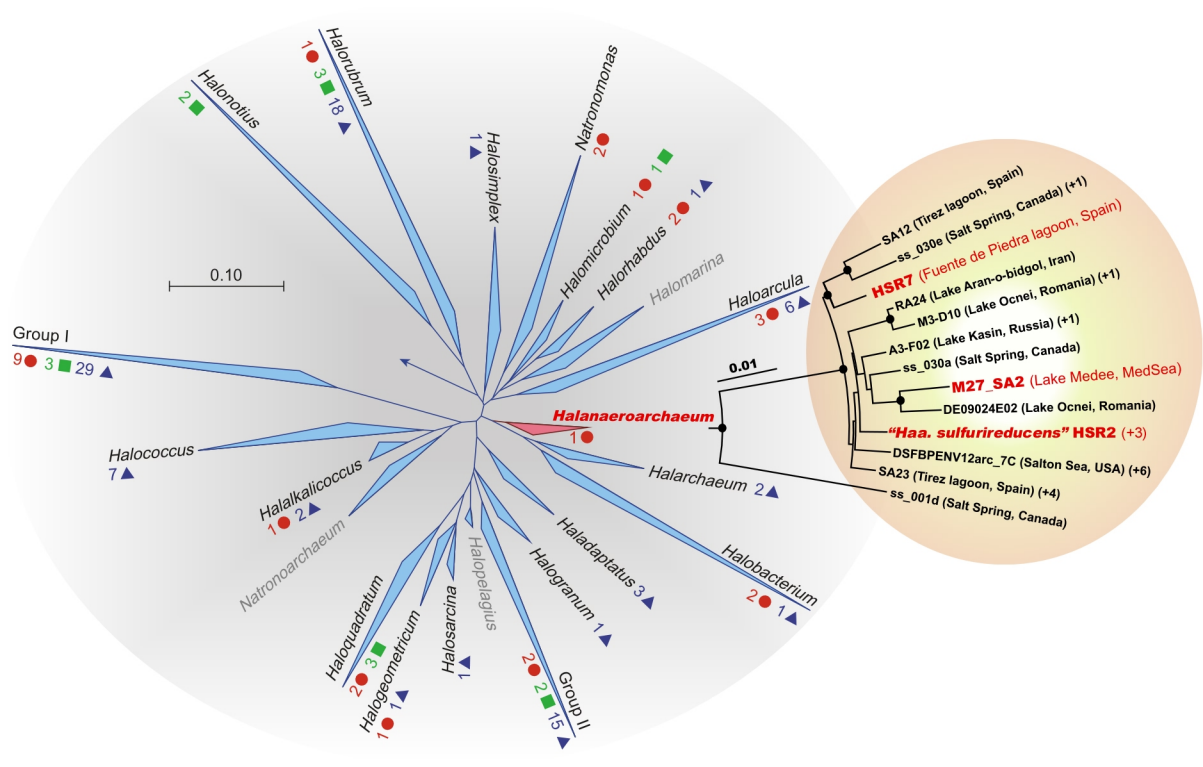
Halorubrum
1 3 18
Halonotius
2
Halosimplex
1
Natronomonas
2
Halomicrobium 1 1
Halorhabdus 2 1
Halomarina
Haloarcula
3 6
0.10
Group I
9 3 29
Halococcus
7
Halalkalicoccus
1 2
Natronoarchaeum
Halanaeroarchaeum
1
Halarchaeum 2
Haladaptatus 3
Halogranum 1
Halopelagius
Haloquadratum
2 3
Halogeometricum
1 1
Halosarcina
1
2 2
Group II
15
Halobacterium
2 1
0.01
SA12 (Tirez lagoon, Spain)
ss_030e (Salt Spring, Canada) (+1)
HSR7 (Fuente de Piedra lagoon, Spain)
RA24 (Lake Aran-o-bidgol, Iran)
M3-D10 (Lake Ocnei, Romania) (+1)
A3-F02 (Lake Kasin, Russia) (+1)
ss_030a (Salt Spring, Canada)
M27_SA2 (Lake Medee, MedSea)
DE09024E02 (Lake Ocnei, Romania)
"Haa. sulfurireducens" HSR2 (+3)
DSFBPENV12arc_7C (Salton Sea, USA) (+6)
SA23 (Tirez lagoon, Spain) (+4)
ss_001d (Salt Spring, Canada)